Figure 1: *Distribution projected onto the galactic plane of those CO emission components associated with the selected IRAS sources. The Sun is at (0,0); the galactic centre at (0,−8.5). The full-drawn lines show the longitude limits of the sample. The dashed lines mark the region within 15° of the anticentre where kinematic distances are very uncertain; objects in this region are excluded from the final sample used in the data analysis.*

than one emission component was found towards a particular IRAS source. Identifying the one that is associated with the IR source usually did not pose a problem, as one of the components was always stronger and broader than the others. Most of the not-associated emission comes from local (d < 1 kpc) clouds.

Figure 1 shows the distribution on the galactic plane of the CO emission associated with the IRAS sources. The dashed lines mark a region near l = 180°, where kinematic distances are very uncertain. Note that very few clouds are at R > 20 kpc. Because the sample was chosen such that the IR sources had colours of star-forming regions, we conclude that no star formation takes place at distances larger than that (otherwise we would have detected it).

We also see that distant objects are found more or less evenly distributed in longitude. There are more molecular clouds with embedded IR sources in the second quadrant than in the third. In the second quadrant a concentration of clouds occurs around R = 12 kpc, which we associate with the Perseus arm. No large-scale spiral arm feature can be distinguished which extends over both galactic quadrants.

The distribution of the CO emission perpendicular to the plane shows that the molecular material partakes in the galactic warp, with clouds reaching heights of 800−1000 pc at the largest

distances. Similarly, the molecular gas disk shows an increase in thickness with increasing R, eventually approaching that of the HI.

Sources that would have a flux S (25 μm) >0.25 Jy if they were at d = 15 kpc, would be visible over the whole range of distances where CO emission was found. Excluding those around l = 180° (see Fig. 1), this sample contains 416 IRAS/CO sources (i.e. molecular clouds), which were used to derive the distribution of $H_2$.

Assuming that the number of far-IR sources per unit of $H_2$ mass is constant (as indicated by a preliminary study), we can derive the surface density of $H_2$ ($\sigma(H_2)$) as a function of R, by calculating the number of IR sources per square pc, and scaling the value at $R_\odot$ with the value of $\sigma(H_2)$ at that location. We find that $\sigma(H_2)$ decreases from a value of 1.80 $M_\odot pc^{-2}$ at the Sun, to 0.64 $M_\odot pc^{-2}$ at R = 14 kpc, to 0.015 $M_\odot pc^{-2}$ at R = 20 kpc. This decrease is much slower than what was derived from earlier, general-sampling CO surveys. From our data, we derive a total mass of 5.8 $10^8$ $M_\odot$ residing in $H_2$ clouds at $R > R_\odot$.

This project shows how the SEST can be used to increase our knowledge of an important aspect of our Galaxy, the large-scale distribution of molecular clouds. The dataset contains of course much more information, which space unfortunately does not permit me to write about; a detailed account of this work has been submitted to *Astronomy and Astrophysics*.

# The Galactic Centre

*Aa. SANDQVIST, Stockholm Observatory, Saltsjöbaden, Sweden*

One of the most interesting and mysterious regions of our Milky Way galaxy is the Galactic Centre (GC). Lying at a distance of 8.5 kpc in the direction of Sagittarius, it is best observed from the southern hemisphere. However, great masses of intervening dust in the plane of the Galaxy produce 30 magnitudes of absorption and the GC is not observable in the optical region. Most of the knowledge that we possess about the GC has been obtained at infrared and radio wavelengths, using northern hemisphere telescopes. These observations are often hampered by the low elevation

of the object, resulting in atmospheric problems and short observing sessions. With its declination of about −30°, the GC becomes almost a zenith object at transit over La Silla and is therefore well suited for studies with SEST.

The inner ten parsecs of the Galaxy contain a giant molecular complex which surrounds the strong continuum radio sources at the nucleus, known collectively as Sgr A. This region somewhat resembles the nuclei of more active galaxies (even to the extent of possibly containing a 3 $10^6$-$M_\odot$ black hole) and its proximity to us is of course a great



The first year of SEST
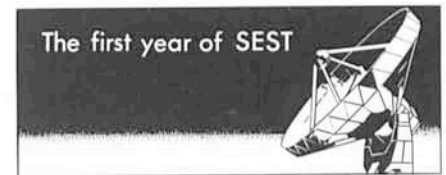
advantage, making possible observations with high spatial resolution. The inner one hundred parsecs of the Galaxy contain more exotic objects, such as continuum threads, filaments and arcs, as well as the most significant star-formation region in the Milky Way, namely Sgr B2.

Four GC projects have been in progress during the first year of SEST and more are in the offing in the near future:
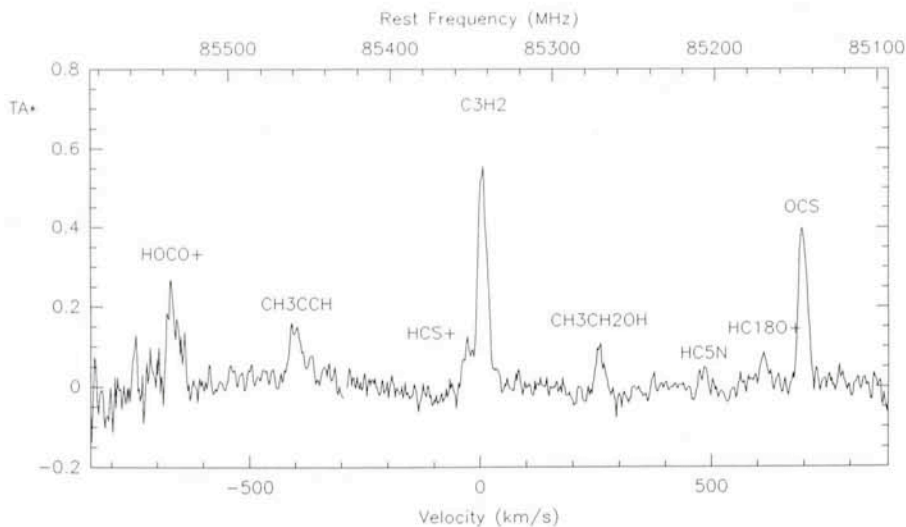
Figure 1: *Part of the spectrum of the Sgr A +20 km s$^{-1}$ molecular cloud covering the frequency range 85.1–85.6 GHz.*

## 1. Physical Conditions in the Sgr A +20 km s$^{-1}$ Molecular Cloud

A research group from Observatoire de Meudon, consisting of N. Bel, M. Gerin, F. Combes and Y.P. Viala, have observed parts of the massive Sgr A +20 km s$^{-1}$ molecular cloud in a large number of molecular lines in the 85–115 GHz frequency range. Figure 1 is an example of one such spectrum

where emission lines from several molecules and molecular ions can be identified, the most intense lines being due to C$_3$H$_2$ and OCS. The centre of the cloud was mapped in $^{13}$CO, C$^{18}$O, HNCO and CH$_3$CN with 40″-spacing. Figure 2 presents maps of integrated line intensities ($\int T_A \cdot dv$) in the velocity range 5–25 km s$^{-1}$. At other frequencies four points were observed roughly along the major axis of the cloud. The

main purposes of the project are to obtain a better insight into the physical conditions and clumpiness of the cloud and to determine the heating source (gravitational collapse, cosmic ray, magnetic heating, gravitational turbulence).

## 2. Prominent Galactic Centre Molecular Clouds

F. Yusuf-Zadeh, M. Lindqvist, J. Bally and L.Å. Nyman have begun a programme of mapping a number of prominent GC molecular clouds (Sgr B, Sgr C, Sgr D, Sgr E) in the 98-GHz J = 2-1 CS and 230-GHz J = 2-1 CO lines. So far, a 10′ × 13′ region around Sgr B1 has been mapped in the CS line with 45″ spacing. The kinematical and spatial distributions of molecular material will be compared with recent 30″-resolution VLA observations of the radio continuum and radio recombination lines. Objectives include determining the reasons for the low rate of massive star formation in the inner few hundred parsecs of the Galaxy (with the exception Sgr B2) and studying the effects of large-scale mGauss magnetic fields.

## 3. A Multitransition CH$_3$CN Study of the Sgr B 22 Molecular Cloud Core

Another group from Onsala Space Observatory, consisting of P. Bergman, P. Friberg and Å. Hjalmarson, is studying the chemical and physical properties of the giant star formation region Sgr B2, which lies about 100 pc from the GC. Sgr B2 has been found to consist of two major cores – Sgr B2 (Main) and Sgr B2 (North) – separated by about two parsecs. The two cores show remarkable differences in their chemical compositions and excitation parameters. Using two multitransitional mapping tools, supplied by the symmetric top molecule CH$_3$CN at frequencies of 110 (J = 6-5) and 220 GHz (J = 12-11), the group expects to derive the temperature structure and heating mechanism in these cloud cores as well as the density structure and CH$_3$CN abundance variations. Figures 3 and 4 show the J = 6-5 CH$_3$$^{12}$CN and CH$_3$$^{13}$CN profiles observed towards Sgr B2 (N) and (M), respectively. From the relative intensities of the different K-components and isotopic lines, it can be deduced that Sgr B2 (N) has considerably higher optical depth and kinetic temperature than Sgr B2 (M).



Figure 2: *Maps of the integrated line intensities in the Sgr A +20 km s$^{-1}$ cloud of a) $^{13}$CO (J = 1-0), b) C$^{18}$O (J = 1-0), c) HNCO (5$_{05}$-4$_{04}$), d) CH$_3$CN (J = 6-5), in the velocity range of 5–25 km s$^{-1}$. RA and DEC offsets are from α (1950) = 17$^h$42$^m$29$^s$.4, δ (1950) = −29°03′31″. Contour levels, in K km s$^{-1}$, are as follows: a) 45 to 100, step 5, bold at 60; b) 5 to 15, step 1, bold at 10; c) 20 to 60, step 5, bold at 40; d) 4 to 60, step 4, bold at 20.*

## 4. Lunar Occultations of Sgr B 2 in the J = 1-0 $^{13}$CO Line

During 1986–1989 a series of lunar occultations of the GC is taking place, a
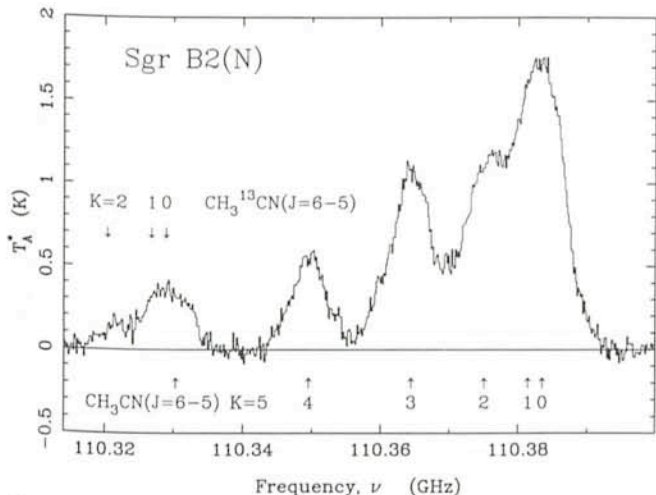
Figure 3: *The line profile of the 110-GHz CH$_3$CN (J = 6-5, K = 0-5) transitions towards Sgr B2 (N).*
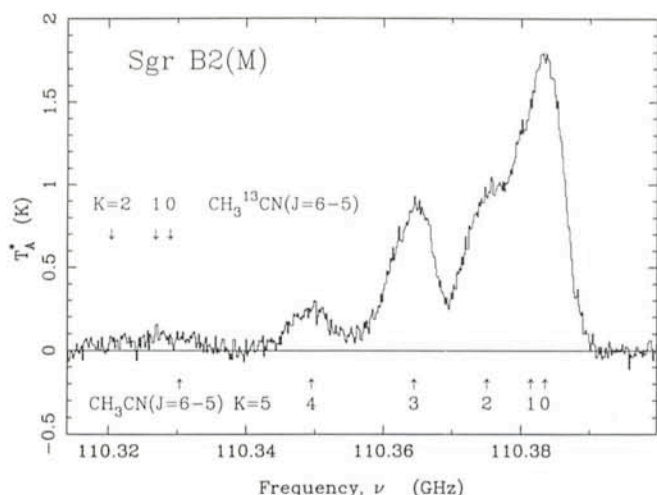
Figure 4: *The line profile of the 110-GHz CH$_3$CN (J = 6-5, K = 0-5) transitions towards Sgr B2 (M).*
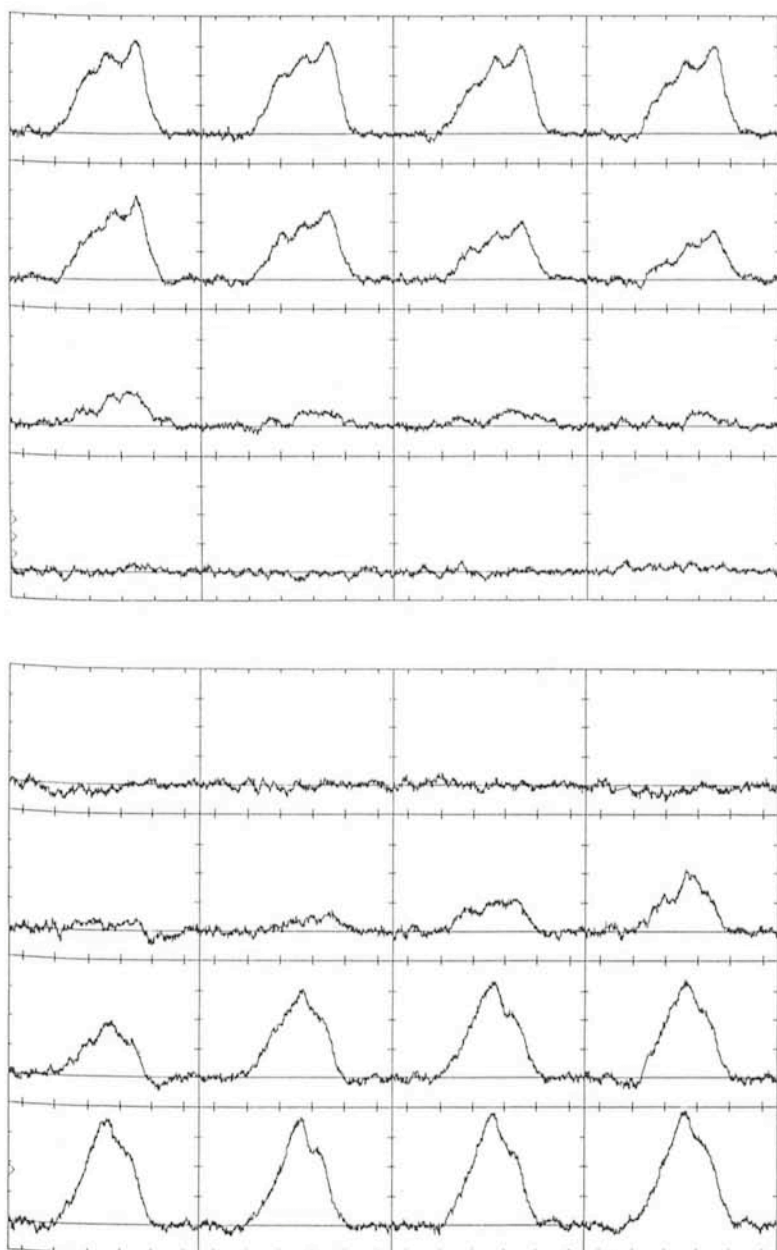




Figure 5: *Variation of the 110-GHz J = 1-0 $^{13}$CO profile during the October 27, 1987 lunar occultation of Sgr B2. The time resolution is 12 seconds. Upper half: disappearance phase of Sgr B2 (M); lower half: reappearance phase of Sgr B2 (N).*
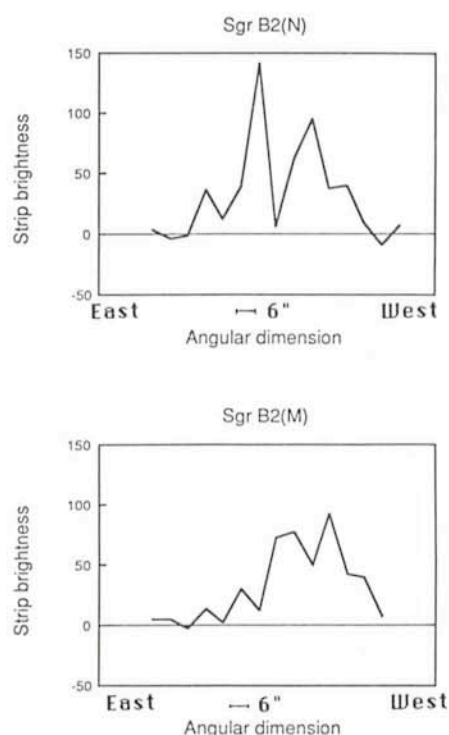


Figure 6: *The restored strip brightness distributions of the integrated line intensity of J = 1-0 $^{13}$CO across Sgr B2 (M) at a position angle of 92°, and across Sgr B2 (N) at a position angle of 250°. The effective angular resolution is 6".*

rare phenomenon. SEST is ideally located for observations of the occultations of Sgr B2 and four occultations have been observed in the 110-GHz J = 1-0$^{13}$CO line by Aa. Sandqvist, L.E.B. Johansson and P. Lindblad. These data can yield the strip brightness distributions along eight different directions across the sources, four for each of Sgr B2 (N) and (M). Figure 5 shows the variation of the $^{13}$CO profile during the disappearance phase of Sgr B2 (M) and the reappearance phase of Sgr B2 (N) on October 27, 1987. The time elapsed be-

tween each dumped profile is 12 seconds, which results in an angular resolution of about 6″. This should be compared with the 46″ beamwidth of SEST at 110 GHz. The corresponding restored strip brightness distributions are seen in Figure 6, showing both sources to be double. The combination of all the strips should yield 5″-resolution maps of the two-dimensional brightness distributions of $^{13}CO$ isotope in Sgr B2 (N) and (M).

# SN 1987 A and other Bolometer Observations at 1.3 mm

*R. CHINI, Max-Planck-Institut für Radioastronomie, Bonn, F. R. Germany*

The first year of SEST

## Introduction

During August/September 1988 the bolometer group of the MPI für Radioastronomie, Bonn, visited SEST to perform continuum observations at 1.3 mm. It was the first observing time of our group at this telescope and the first sensitive test for SEST at that wavelength. The submm qualities of La Silla were another uncertainty in the mission so that it seemed more than questionable whether any astronomical data would come out of our run.

We started on August 24 to install our bolometer in the receiver cabin of the telescope. This action turned out to be quite an adventure because the access to the cabin door – 9 m above the ground – is only possible from outside via a ladder or a hydraulic platform (cherry picker). During the observing run we had to use the "cherry picker" each day in order to take the cryostat with the bolometer from the telescope, bring it back to the ground and refill with Helium. The ladder was also used very often because receiver alignments and all kind of trouble-shooting in the cabin had to be interrupted at least four times a day to experience La Silla's famous cuisine.

## Sub-Millimetre Observing Conditions

The sub-mm-transparency of the atmosphere is – as in the infrared spectral region – confined to a few windows. Most of the radiation is absorbed by the water vapour content of the atmosphere so that dry sites of high altitude are ideal for observations of that kind. The first measurements of the atmospheric transmission on La Silla at 1.3 mm with SEST were quite surprising because we faced conditions as good as those on the 4200 m volcano Mauna Kea in Hawaii, the world's most famous sub-mm site. However, the joy lasted for only a few hours and then we had – despite blue skies – 9 days of only moderately good sub-mm observing weather. Together with the SEST team we used this time to test various properties of the

telescope like pointing, tracking and the accuracy of the 15 m diameter surface. The short observing wavelength of 1.3 mm and the superior sensitivity of our bolometer system enabled us to detect telescope errors much more efficiently than with existing receivers at SEST. We located encoder problems which caused tracking errors and found a misalignment of the subreflector that distorted the beam shape.

Unfortunately, SEST was not yet equipped to record our continuum data by the telescope computing system and no on-line reduction of the signals was possible. Likewise, our own PC data acquisition was too busy with taking data so that the strip chart records were the only way of monitoring the observations. Just as we had finished the technical tests and had most of our problems under control, heavy clouds came in and stopped further astronomical activities during the next 4 days. This was the opportunity to summarize our experience with SEST and to discuss further observations that could be reasonably done with the present state of the system. The telescope performance had turned out to be still inferior to what it was supposed to be; any efficient observing procedure was extremely difficult because of the lack of corresponding on-line reductions. Daytime observations were severely limited by an increased turbulence of the atmosphere which resulted in an overall sensitivity-loss of the system. In addition, the reflecting aluminium surface of the telescope had once burnt the subreflector, so we had to avoid the sun by an angle of 60 degrees and, as a consequence, could not reach many interesting objects. In view of all these limitations, the bad weather and the knowledge that only a few days of telescope time were left, a feeling of disappointment set in whenever the dining room was closed.

## Observations – At Last!

Finally, it cleared up, the relative humidity dropped below 15% and the average temperature fell to 3°C, much

below the previous values. During the last three days we experienced excellent sub-mm conditions and started with astronomical observations. To observe faint sources with a radio or a sub-mm telescope it is essential to determine the pointing of the telescope by means of nearby strong sources with well-known positions. For that purpose we observed a sample of quasars well distributed across the southern hemisphere and selected those which were strong enough at 1.3 mm, to establish a system of pointing calibrators.

It must be noted of course that all these measurements were new for the southern hemisphere and tell quite a lot about the physical properties of the quasars: Their 1.3 mm radiation is due to fast moving electrons (synchrotron radiation). From the intensity of the emission (in combination with other radio data) one can learn about the energy of the electrons, the strength of the magnetic fields and even about the size of the emitting regions.

The sub-mm emission of most other objects, however, is – as in the near and far infrared spectral region – thermal in origin and comes from interstellar dust that is heated by nearby stars. In particular, star-forming regions are strong emitters of sub-mm radiation because young stars there are deeply embedded in dust clouds. The light at optical and infrared wavelengths is completely absorbed by dust and is re-radiated at longer, i.e. at far-infrared and sub-mm wavelengths. Thus, sub-mm emission is very often the only sign for star formation occurring in dense clouds.

Even more interesting is the search for "protostars", i.e. cool and dense objects of gas and dust which are still in a phase of gravitational contraction. Here it seems that sub-mm observations are the most promising way to detect these cool ($\approx 20$ K) precursors of stars. We mapped several well-known southern star-forming regions to determine the amount of gas and dust associated with them and to look for condensations which might develop into stars in the future.

18